JOURNAL OF MATERIALS SCIENCE 10 (1975) 2082–2091

Effect of frictional forces on the behaviour of dislocation loops

K. SADANANDA
Engineering Materials Group, and Department of Mechnical Engineering, University of Maryland, College Park, Maryland, USA

A detailed analysis of the effect of frictional forces on the stability of dislocation loops lying in their glide planes and the effect of these forces on the cross-slip behaviour of these loops under both applied stresses as well as internal stresses arising from other dislocation loops, has been made. In addition, the passing as well as cross-slip behaviour of non-coaxial dislocation loops has been analyzed and it is shown that these loops could give rise to Frank–Read sources by way of cross-slip; and the conditions for generations of such Frank–Read sources have been determined. The results show that depending upon strain, the cross-slip of dislocation loops could lead to regeneration of dislocation and subsequent work-hardening, or to dynamic recovery or stage III deformation. The significance of the above results in relation to the behaviour of dislocation loops observed in real crystals is discussed in detail.

1. Introduction

It has been previously shown [1] that frictional forces are of great importance in stabilizing many dislocation configurations which are otherwise unstable. Such configurations include, for example, two or more like dislocations on the same slip plane or two or more dislocation dipoles on parallel slip planes, etc. Since there are only repulsive forces between the dislocations in these configurations, they tend to separate to infinity if there are no frictional forces present. The importance of frictional forces was also demonstrated for passing coaxial dislocation loops [2]. In particular, it was shown that frictional forces lock the expanding loop in preference to the contracting one, whereas the absence of such forces would cause both loops to collapse simultaneously, even in the presence of an applied stress, in order to lower the self energy of the loops. Due to their irreversible nature, frictional forces also induce a strain history dependence [1] with respect to the equilibrium configurations of various dislocation arrays, thus influencing the dislocation substructure and hence the mechanical properties of many crystals.

In the following sections, we shall further examine the effect of frictional forces on the stability of dislocation loops. It has been shown, recently [3] that unextended dislocation loops could spontaneously cross-slip or double cross-slip in the presence of an applied stress. If there are no frictional forces present, these cross-slipped loops could expand continuously in their cross-slipped configuration without giving rise to Frank–Read sources [4]. On the other hand, it would be possible for dislocation loops to generate Frank–Read sources, if frictional forces were present, which could selectively lock some of the segments of the loops while the others can still move under the applied stress. The conditions for the loops to become Frank–Read sources by way of cross-slip or double cross-slip [5] will be examined and will be discussed in the light of many experimental results [6–9] which seem to give credence to the thesis [6] that cross-slip of dislocation loops is a prerequisite for them to act as Frank–Read sources.

2. Stability of a single dislocation loop

In the absence of frictional forces, a dislocation loop in an otherwise perfect crystal becomes unstable. Under a constant applied stress, the loop either collapses, if its size is less than some critical size, or else it expands to infinity, if its size is greater than some critical size. Because of the differences in self energies of screw and edge dislocations, the dislocation loop, in general, is of elliptical shape [10] with the ratio of the major to minor axis of the ellipse of the order of $1/(1-\nu)$, where ν is Possion's ratio. Without any loss of generality, the analysis of these loops is simplified here by approximating them in terms of piecewise segments [11]. In particular, an elliptical loop is approximated by a rectangular loop, with R_1 and R_2 defining the size of the loop (Fig. 1a). For a given applied stress, the critical size of such a loop corresponds to a saddle point [3] in the total energy surface, with the energy maximum with respect to R_2 and minimum with respect to R_1.

The dashed line in Fig. 2 corresponds to the variation of the critical size of the loop with applied stress. While the figure shows only the variation of R_1 with stress, R_2 also varies proportionately with R_1 and a detailed discussion of the equilibrium configuration of the loops with stress is presented elsewhere [3]. Of interest at present, however, is the effect of frictional force on the equilibrium size of the loop. The change in the total energy of a loop as it moves from some reference configuration, R, is given by

$$\Delta E_{\mathrm{T}} = (E_{\mathrm{S}} - E_{\mathrm{S}}^{\mathrm{R}}) - \tau_{\mathrm{a}} \boldsymbol{b}(A - A^{\mathrm{R}}) + |\tau_{\mathrm{f}} b(A - A^{\mathrm{R}})| \tag{1}$$

Where E_{S} is the self energy of the loop, τ_{a} the applied stress, τ_{f} the frictional stress, $\boldsymbol{b}$ the Burgers vector, and A the area of the loop. The superscript R denotes the reference configuration. The absolute value in the above expression takes into consideration the irreversibility of frictional forces, which makes them always positive. For a loop continuously expanding from zero radius, the above expression reduces to

$$E_{\mathrm{T}} = E_{\mathrm{S}} - (\tau_{\mathrm{a}} - \tau_{\mathrm{f}})\boldsymbol{b}A \tag{2a}$$

which indicates that the equilibrium size of an expanding loop can be easily obtained by translating the dashed curve in Fig. 2 to the right by τ_{f} units. Likewise, if the loop is continuously contracting from some large radius R, then the change in the total energy of the loop is given by

$$\Delta E_{\mathrm{T}} = \Delta E_{\mathrm{S}} + (\tau_{\mathrm{a}} + \tau_{\mathrm{f}})\boldsymbol{b}(A^{\mathrm{R}} - A) \tag{2b}$$

implying that the equilibrium size of such a contracting loop can be obtained by translating the dashed curve in Fig. 2 to the left by τ_{f} units. To be more specific, the two solid lines in Fig. 2 represent the two limiting equilibrium configurations of a dislocation loop depending upon the direction of motion of the loop. These limiting equilibrium configurations are somewhat similar to those discussed earlier for infinite dislocation lines [1]. Furthermore, while the two solid curves describe the unstable equilibrium configurations of the loops (saddle point equilibrium), the region in between these two curves represents the stable equilibrium configurations, i.e. with energy minimum in terms of both variables, R_1 and R_2. Such equilibrium configurations were termed friction induced stable equilibrium configurations [1]. Clearly, the range of stability of the loops depends on the magnitude of the frictional stress; and it approaches zero as the frictional stress goes to zero In terms of the line tension of the loop, the stability of the loops can be represented by the following inequality for an applied stress:

$$\tau_{\mathrm{L}} - \tau_{\mathrm{f}} \leqslant \tau_{\mathrm{a}} \leqslant \tau_{\mathrm{L}} + \tau_{\mathrm{f}} \tag{3}$$

where the equality signs correspond to the points on the two solid curves in Fig. 2 and thus refer to unstable equilibrium. Physically, this means that if

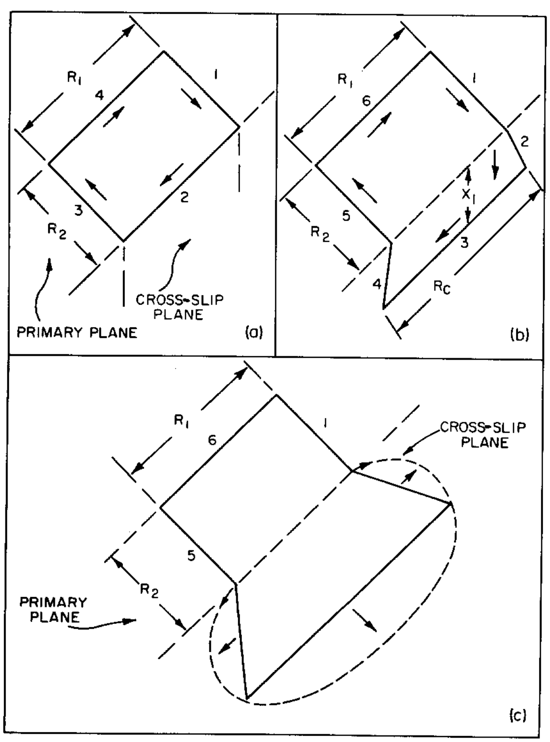

Figure 1 Schematic illustration showing a dislocation loop (a) before cross-slip, (b) during cross-slip, (c) cross-slipped loop acting as a Frank–Read source for dislocations on the cross-slip plane.

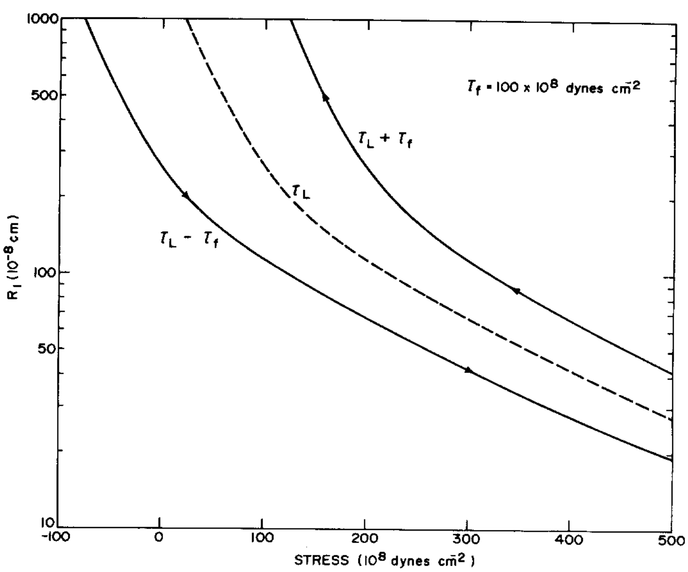

Figure 2 Equilibrium configurations of a single dislocation loop in the presence of frictional forces.

the applied stress is less than $\tau_L - \tau_f$, then the line tension of the loop, τ_L, is greater than the total opposing forces due to the applied stress and frictional stress hence the loop collapses. On the other hand, if the applied stress is greater than $\tau_L + \tau_f$ the loop expands to infinity. In between the two limits, the total force on the loop is neither sufficient to expand the loop nor sufficient to collapse the loop and hence the loop becomes stable in this range.

3. Cross-slip of dislocation loops

Fig. 1b represents the piecewise approximation of a dislocation loop during its asymmetric cross-slip. The stresses acting on the loop are denoted by τ_{ap} and τ_{fp}, and τ_{ac} and τ_{fc}, where the first two stresses are the applied and frictional stresses on the primary plane while the last two are the corresponding stresses on the cross-slip plane. The change in the total energy of the loop as it cross-slips from some reference configuration (Fig. 1a) is given by

$$\Delta E_T = \Delta E_S - \tau_{ap} b(A - A^R) + |\tau_{fp} b(A - A^R)| - (\tau_{ac} - \tau_{fc}) b X_1 R_1 . \quad (4)$$

The expression for the self energy of the loop in the piecewise approximation is given by

$$\Delta E_S = 2(E_{SC}^1 + E_{SC}^2 + E_{SC}^3 - E_S^1 - E_S^2) + 2E_{IC}^{1-2} + 2E_{IC}^{1-4} + E_{IC}^{2-4} + (E_{IC}^{1-5} - E_I^{1-3}) + (E_{IC}^{3-6} - E_I^{2-4}) \quad (5)$$

where E_{SC}^i is the self energy of segment i and E_{IC}^{i-j} is the interaction energy between segments i and j. The additional subscript C corresponds to the corresponding energies in the cross-slip configuration (Fig. 1b). All of the above energies are obtained by using the expressions developed by Jossang and his co-workers [12, 13]. If the applied stress on the primary plane falls in between the solid curves in Fig. 2, the loop on the primary plane is stable with respect to expansion or contraction on the primary plane. It is however, free to cross-slip if the applied stress on the cross-slip

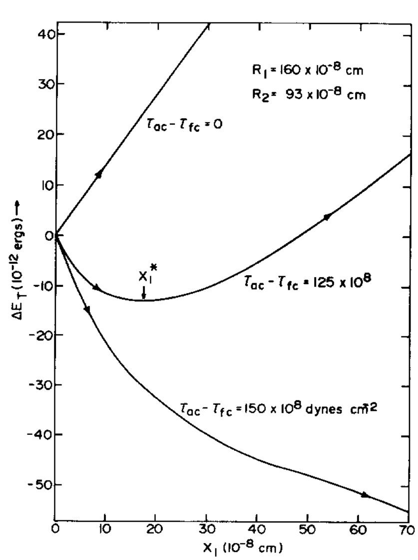

Figure 3 Change in the total energy of a cross-slipping dislocation loop as a function of its cross-slip distance in the presence of frictional forces.

plane is greater than the frictional stress on that plane. Typical results for an initial loop size of $R_1 = 163 \times 10^{-8}$ cm and $R_2 = 93 \times 10^{-8}$ cm as well as $\tau_{ap} = 150 \times 10^8$ dyn cm^{-2} and $\tau_{fp} = 100 \times 10^8$ dyn cm^{-2} are presented in Fig. 3. This figure shows that for an applied stress less than or equal to the frictional stress, no significant cross-slip of the loops occur* and the cross-slip energy monotonically increases with cross-slip distance. For the stresses greater than the frictional stress, say when $\tau_{ac} - \tau_{fc} = 125 \times 10^8$ dyn cm^{-2}, the loop spontaneously cross-slips to a distance X_1^* corresponding to the minimum in the $\Delta E_T - X_1$ curve in Fig. 3. During this cross-slip processes, the size of the loop on the primary plane remains unchanged due to the presence of frictional forces on that plane. The equilibrium configuration of the cross-slipped loop ($X_1^* = 17.5 \times 10^{-8}$ cm), however, is not significantly different from that obtained [3] for $\tau_{ac} = 125 \times 10^8$ dyn cm^{-2} when there are no frictional forces present on either plane. On the other hand, for a larger stress, say for $\tau_{ac} - \tau_{fc} = 150 \times 10^8$ dyn cm^{-2}, there is no energy minimum in Fig. 3, and instead, the energy continuously decreases with X_1. Two possibilities arise here. The loop on the cross-slip plane can expand indefinitely without the corresponding expansion of the loop on the primary plane. Such an expansion would give rise to Frank–Read source for dislocations on the cross-slip plane such as shown in Fig. 1c. Otherwise, the cross-slipped loop could force the primary loop to expand along with it due to its line tension and the results in that case would converge to those obtained earlier when there were no frictional forces present. In order for the cross-slipped loop to act as a Frank–Read generator, the frictional forces on the primary plane should be of sufficient magnitude to overcome the line tension discussed above.

The following procedure is adopted for the determination of the approximate value of the frictional stress. The loop on the cross-slip plane is defined by X_1 and R_C, where R_C is the length of the screw segment of the cross-slipped loop (Fig. 1b) which could be different from R_1 if the loop on the cross-slip plane expands independently of the loop on the primary plane. For the cases where R_C differs from R_1, an additional energy term $2(E_{IC}^{2-3} + E_{IC}^{2-6})$ should be added to the self energy expression in equation 5 and simultaneously the last term in Equation 4 alters to $-(\tau_{ac} - \tau_{fc})\boldsymbol{b}\{X_1 R_1 + (R_C - R_1)X_1\}$. The contribution from the above interaction energy terms vanishes when $R_C = R_1$ since the interaction energy between pure screw and pure edge dislocation segments is zero. It is found that for frictional stresses, τ_{fp}, greater than or equal to the line tension of the initial loop, τ_L (Fig. 2), R_1 and R_2 remain at the stable equilibrium (with energy minimum) for all values of R_C and X_1. Hence the frictional stress of this magnitude is sufficient to overcome any line tension on the primary plane due to expanding loop on the cross-slip plane. For a frictional stresses less than the line tension of the initial loop, R_C and R_1 remain equal until X_1 attains the order of R_2 (for $X_1 = R_2$ the loop is symmetrically distributed in both planes), and R_C and R_1 both increase indefinitely for any further increase of X_1 beyond the symmetry configuration. Hence for these frictional stresses, the behaviour of the loop is similar to that reported earlier [3] for zero frictional stress. Also, it is found that when the loop on the primary plane remains stable in the presence of frictional forces, spontaneous double cross-slip of the loop, such as was reported earlier [3], does not occur. This is again due to the fact that the applied stress on that plane is less than the opposing forces of the frictional stress and the line tension of the loop.

4. Non-coaxial dislocation loops

We shall next turn our attention to the behaviour of non-coaxial dislocation loops which pass one another on parallel slip planes in the presence of frictional forces. The behaviour of coaxial dislocation loops in the presence of frictional forces has already been treated earlier [2]. Since the dislocation loops in a real crystal nucleate at various points inside the crystal and expand until they meet one another, the analysis of the behaviour of such non-coaxial dislocation loops is of particular interest in relation to the work-hardening behaviour of metals and alloys.

4.1. Passing behaviour

It was reported earlier [14] that in the absence of

*The screw segments of a dislocation loop could cross-slip by thermal activation even when the applied stresses are less than the frictional stresses. The analysis of this thermally activated cross-slip, however, is beyond the scope of the present analysis.

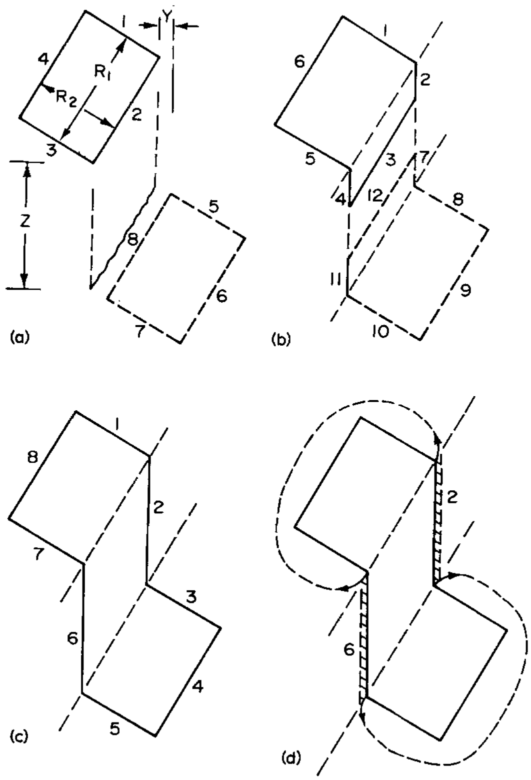

Figure 4 A schematic illustration showing two non-coaxial passing dislocation loops on parallel slip planes (a) before cross-slip, (b) during cross-slip, (c) after cross-slip and annihilation, (d) cross-slipped loops acting as Frank–Read sources for dislocations on the primary planes.

frictional forces two non-coaxial dislocation loops on parallel slip planes in an otherwise perfect crystal do not pass one another. Instead, segments of the loops that face each other form dipoles, while the rest of the loops expand continuously on their respective planes. Fig. 4a shows two such non-coaxial dislocation loops approaching one another with their screw segments facing each other. For a given applied stress, $\tau_{ap} = 150 \times 10^8$ dyn cm^{-2}, the total energy of the equilibrium size of the loops (saddle point equilibrium) is determined and represented in Fig. 5 as a function of their separation, Y, and for various selected values of Z. When $Y \rightarrow \infty$, the two loops behave independently of each other and the total energy of the two loops approaches a constant corresponding to twice the energy of each loop. As Y decreases, the interaction between the two loops becomes significant and the energy reaches a minimum for Y very nearly equal to zero so that correspondingly the unlike segments of loops, i.e. 2 and 8, form a dipole. For a further decrease of Y below zero, which corresponds to the passing of dislocation

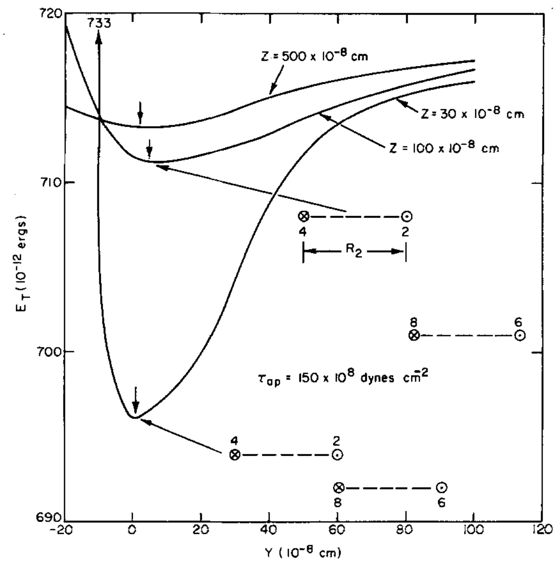

Figure 5 Total energy of two non-coaxial dislocation loops as a function of their separation and for various selected values of Z.

loops over one another, Fig. 5 shows that the energy increases very fast indicating that such passing is energetically unfavourable. While the minimum in the total energy at $Y \approx 0$ exists for any value of Z, it becomes increasingly shallow with increasing Z; so that when $Z \rightarrow \infty$, the two loops can be considered as independent of one another and the total energy of such loops remains nearly constant for all values of Y. Also of interest to note in Fig. 5 is that the equilibrium value of Y (Y at the energy minimum) attains a maximum value when Z is of the order of R_2, since for this configuration the repulsive forces between segments 4 and 8 are a maximum [4].

It is found that the presence of frictional forces does not affect the behaviour of two non-coaxial dislocation loops in an otherwise perfect crystal. Identical E_T–Y cruves (Fig. 5) were obtained when the applied stress is replaced by $(\tau_{ap} - \tau_{fp}) = 150 \times 10^8$ dyn cm^{-2}. Since the frictional forces are assumed to be uniform on all segments of the loop, the dislocation loops expand continuously on their glide planes with one end of each loop locked as a dipole.

4.2. Mutual cross-slip

It was shown earlier [14] that spontaneous cross-slip of non-coaxial dislocation loops occurs under their own internal stresses and such cross-slip leads to the annihilation of the unlike screw segments of the two loops and hence to the dynamic

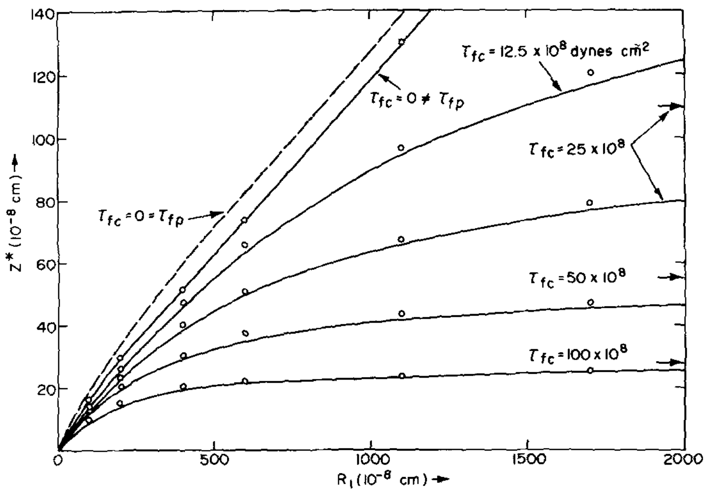

Figure 6 Variation of Z^* with dislocation loop size for various frictional stresses on the primary and cross-slip planes.

recovery. For such cross-slip to occur, the interplanar separation of the loops, Z, should be less than some critical value, Z^*, so that the internal stresses are of sufficient magnitude to overcome the forces of the line tension of the two loops. The dashed line in Fig. 6 shows the result of the previous calculation [14] where there are no frictional forces on both the primary and cross-slip planes. In the presence of frictional forces, however, the change in the total energy during mutual cross-slip is given by

$$\begin{aligned} \Delta E_{\mathrm{T}} &= \Delta E_{\mathrm{S}} + \Delta E_{\mathrm{I}} - 2\tau_{\mathrm{ap}} b(A - A^{\mathrm{R}}) \\ &\quad + 2|\tau_{\mathrm{fp}} b(A - A^{\mathrm{R}})| + 2|\tau_{\mathrm{fc}} b X_1 R_1|. \end{aligned} \tag{6}$$

It is next assumed for simplicity that there are no applied stresses on the cross-slip plane and further that mutual cross-slip begins to occur after the loops reach equilibrium on their primary plane, i.e. with Y equal to zero (Figs. 4 and 5). When there are frictional forces present on the primary plane, the contribution from the 3rd and 4th terms on the right hand side of the above equation vanishes since the size of the loops on the primary plane remain unaltered during the entire cross-slip processes. In such cases, the change in the self energies of the two loops, ΔE_{S}, and the interaction energy between the two loops, ΔE_{I}, reduce to

$$\begin{aligned} \Delta E_{\mathrm{S}} &= 4E_{\mathrm{SC}}^{2} + 2E_{\mathrm{I}}^{2-4} + 4E_{\mathrm{IC}}^{1-2} + 4E_{\mathrm{IC}}^{1-4} \\ &\quad + 2(E_{\mathrm{IC}}^{3-6} - E_{\mathrm{I}}^{2-4}) \end{aligned} \tag{7a}$$

and

$$\begin{aligned} \Delta E_{\mathrm{I}} &= 4E_{\mathrm{IC}}^{1-7} + 4E_{\mathrm{IC}}^{1-11} + 2E_{\mathrm{IC}}^{2-7} \\ &\quad + 2(E_{\mathrm{IC}}^{3-9} - E_{\mathrm{I}}^{2-6}) \\ &\quad + (E_{\mathrm{IC}}^{3-12} - E_{\mathrm{I}}^{2-8}) \end{aligned} \tag{7b}$$

where again E_{S}^{i} and E_{I}^{i-j} correspond to self energy of segment i and interaction energy between segments i and j, respectively in the uncross-slipped configuration (Fig. 4a) and E_{SC}^{i} and E_{SC}^{i-j} are the respective energies in the cross-slipped configuration (Fig. 4b). While the exact expression for each one of the interaction energy terms is quite complicated, it is possible to write an approximate expression for the total energy given by Equation 6 in the following form after some lengthy algebriac manipulation and after neglecting terms such as E_{IC}^{1-4}, E_{IC}^{2-4} etc. which have only second order effects on the total energy of the loops.

$$\begin{aligned} \Delta E_{\mathrm{T}} &\approx \frac{\mu b^2}{4\pi(1-\nu)} 4X_1 \left\{ \ln\left(\frac{X_1}{r_0}\right) + (3-\nu) \right. \\ &\quad \left. - \frac{R_1(1-\nu)}{Z} \right\} + 2\tau_{\mathrm{fc}} b X_1 R_1 \end{aligned} \tag{8}$$

where the first term inside the brackets corresponds to the contribution of self energy of each edge segment (segments 2, 4 etc.) and the last term is the change in the interaction energy between segments 3 and 12 as they glide towards each other on the cross-slip plane. Since the energy barrier for cross-slip disappears when $Z = Z^*$, the above equation can be solved for Z^* by equating it to zero and hence Z^* is given by

$$Z^* \approx \frac{R_1(1-\nu)}{\left[\left\{\ln\left(\frac{X_1}{r_0}\right)+(3-\nu)\right\}+\frac{\tau_{fc}R_1 2\pi(1-\nu)}{\mu b}\right]} \tag{9}$$

where r_0 is core radius. Like in the previous analysis all of the present calculations are done using the material constants corresponding to FeCo alloy [15]. In particular, $\mu = 7 \times 10^{11}$ dyn cm^{-2}, $\boldsymbol{b} = 2.47 \times 10^{-8}$ cm and $\nu = \frac{1}{3}$ have been used.

Fig. 6 shows the variation of Z^* with the loop radius for various selected values of frictional stresses. The datum points in this figure correspond to the computer calculations employing the exact expressions for the total energy (Equations 6 and 7) and using the numerical techniques discussed earlier [14]. For Z close to Z^*, these calculations showed that the instability of the two loops with respect to continuous cross-slip occurs when X_1 was on the order of 5×10^{-8} cm. This is related to the fact that the internal stresses increase very fast with X_1 [14] especially when Z is close to Z^*. Substituting this value for X_1 in Equation 9, the values of Z^* was determined as a function of R_1 and these results are represented in Fig. 6 by the continuous curves. Since X_1 occurs in the log term in Equation 9, it can be shown that Z^* is quite insensitive to the exact value of X_1 and is even more so when the loop size is large.

The straight, solid line in Fig. 6 corresponds to the case where $\tau_{fc} = 0$ and $\tau_{fp} \neq 0$. Since the presence of frictional stress on the primary plane induces regidity for the loop on that plane, Z^* for this case differs slightly from the case where both frictional stresses are absent (dashed line). In both cases, however, Z^* increases to infinity as $R \to \infty$ implying that for infinite dislocations spontaneous cross-slip occurs for any value of Z and this is related to the absence of any opposing frictional forces on the cross-slip plane. On the other hand, when there are frictional forces present on the cross-slip plane, Z^* approaches a limiting value as $R_1 \to \infty$; and this limiting value of Z^* decreases very rapidly with an increase in frictional stress. From Equation 9, this limiting value of Z^* is given by

$$Z^*_{max} = \frac{\mu b}{2\pi\tau_{fc}} \tag{10}$$

which could also be obtained independently by balancing the interaction forces between two parallel infinite dislocations against the frictional force on the cross-slip plane. Clearly, as $\tau_{fc} \to 0$, $Z^*_{max} \to \infty$ as discussed above. It should also be mentioned here that the above results (Fig. 6) can be used even when there is an applied stress on the cross-slip plane except in this case τ_{fc} in Fig. 6 is now replaced by $(\tau_{fc} - \tau_{ac})$ which gives the frictional stress which is over and above the applied stress.

4.3 Frank–Read sources

After the cross-slip and mutual annihilation of the unlike screw segments of the loops, the configuration of the loops reduce to that shown in Fig. 4c. The next question to ask is how such a loop will expand further under the action of the applied stress on the primary plane. Again two possibilities exist. The loops on the primary planes could expand continuously on their respective planes dragging the edge segments 2 and 6 (Fig. 4c) along with them by their line tension. In such a case the results would converge to those where there are no frictional forces present. On the other hand, edge segments 2 and 6 could remain stationary due to frictional forces which are greater than the tension exerted by the loops on the primary plane; and in which case continuous expansion of the loops on the primary plane could give rise to Frank–Read sources for dislocations on these planes, as shown in Fig. 4d. The magnitude of frictional stress necessary to hold the edge segments stable can be estimated by using the following approximate equation for the change in the total energy as the edge segments move by a distance b on their glide plane (Fig. 4d).

$$\Delta E_T \approx \frac{\mu b^2}{4\pi}\left\{-2b\ln\frac{b}{r_0}+\frac{2Zb}{R(1-\nu)}\right\}+|\tau_f bZ\cdot b|, \tag{11}$$

where the first term inside the brackets represents the reduction in the energy as each edge segment moves a distance b, since such a motion involves the elimination of two unlike screw segments each of length b (Fig. 4d) while the second term is the work done to overcome the attractive forces between the two edge segments. Finally, the last term in the above equation is the frictional energy. The magnitude of τ_f can be estimated by equaling the above expression to zero and is given by

$$\tau_f^* = \frac{\mu b}{2\pi Z}\left\{\ln\left(\frac{b}{r_0}\right)-\frac{1}{R(1-\nu)}\right\}. \tag{12}$$

Equations 9 and 12 can both be solved simultaneously for τ_f^* and Z^* for various loop sizes and the solutions of these equations represent the conditions (Z^* and τ_f^*) necessary for two non-coaxial dislocation loops on parallel slip planes to mutually cross-slip under their own internal stresses and to further expand on their primary planes so as to give rise to Frank–Read sources on these planes. The values of Z^* and τ_f^* thus obtained are represented in Fig. 7 as a function of the loop size. For reasonable values of frictional stresses that are normally encountered in real crystals ($\tau_f = 15 \times 10^8$ dyn cm^{-2} for Fe–3% Si [8], Fig. 7 shows that for the dislocation loops to act as Frank–Read sources, the loop size (R_1) as well as the length of the jogs (Z^*) should be very large. While the above two conditions present the size of the loops and the spacing between them, for the loops to act as Frank–Read sources, they should also be able to pass one another [8], and therefore the applied stress should be greater than the passing stress which in the infinite line approximation is of the order of $\mu \boldsymbol{b}/(2\pi Z)$. It should also be mentioned here that the results of Fig. 7 can be used even when there is an applied stress, τ_{ac}, on the cross-slip plane. In such case τ_{fc}^* in Fig. 7 is replaced by ($\tau_{fc} - \tau_{ac}$) that is the magnitude of frictional stress which is over and above the applied stress.

5. Discussion

The above analysis clearly shows that frictional forces can significantly effect the stability of dislocation loops. their passing as well as their cross-slip behaviour, and finally their ability to act as Frank–Read sources for dislocations in the primary as well as cross-slip planes. It is next important to analyse the significance of these results in relation to the behaviour of dislocation loops in real crystals.

Experimental results on single crystalline Fe–3% Si alloys [8] as well as on many other metals and alloys that have relatively high stacking fault energy [16–24] show that most of the screw dislocations are heavily jogged and that the motion of these jogged dislocations generate edge dipoles or dipoles of near edge orientation. This jogging of screw dislocations and the subsequent formation of edge dipoles has been attributed, among many other things, to the cross-slip of screw dislocations [8]. Since only parts of the screw dislocation lines have cross-slipped rather than the complete lines, the major driving force for such a cross-slip should be the internal stresses rather than the applied stress.

Tetelman [25] has proposed a different model to account for the formation of edge dipoles. In particular, he showed that passing dislocations on parallel slip planes could rearrange partly into edge dipole configuration to lower their energy. Such a rearrangement would also leave the rest of the segments of the dislocations as pure screw dislocations, the subsequent cross-slip of which results into the jog formation. While this model is attractive since it is based on the experimental observations which show the presence of equal number of dislocations of both signs on parallel slip planes, his calculations seems to suggest that such a rearrangement to give rise to edge dipoles is most energetically favourable when the passing dislocations are predominantly of edge character.

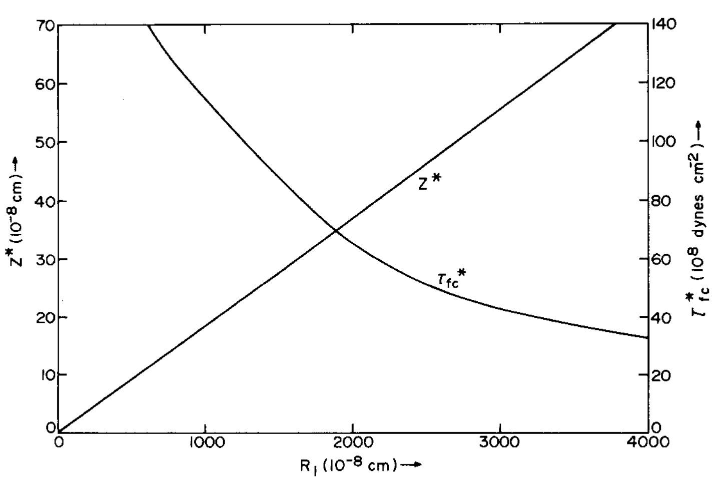

Figure 7 Variation of Z^* and τ_f^* as a function of loop size for two non-coaxial dislocation loops.

On the other hand, the experimental results [8] show that dislocations are predominently of screw type. Also, while the above model still assumes the cross-slip of screw segments for the formation of jogs, the driving force for such cross-slip is left unaccounted for.

In the following a model somewhat similar to that of Tetelman [25] is proposed taking into consideration the presence of predominent number of screw dislocations in the real crystal which are likely to form screw dipoles rather than edge dipoles. Fig. 8a, for example, schematically shows non-coaxial dislocation loops with large screw segments that one could encounter in a real crystal. When the dislocation loops meet one another, the screw segments of the loops could form dipoles. Mutual cross-slip of the dislocation loops could occur under their own internal stresses leaving edge jogs such as shown in Fig. 8b. The applied stress on the primary plane could bow out the remaining screw segments giving rise to edge dipoles, Fig. 8c. In contrast to Fig. 4d, the adjacent bowed out segments at each jog in Fig. 8c induce forces of opposite sign and hence the jogs may be stable with respect to lateral glide. Since these forces would depend on the lengths l_1 and l_2 etc. (Fig. 8c), the resulting dipoles need not always be of pure edge orientation in agreement with the experimental results.

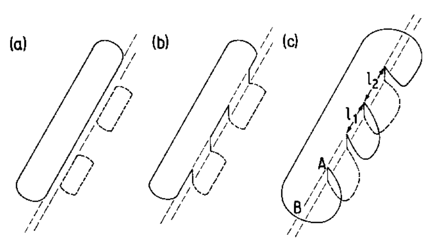

Figure 8 Schematic illustration showing the interaction of non-coaxial dislocation loops in a real crystal (a) before cross-slip, (b) mutual cross-slip and annihilation of unlike screw segments, (c) formation of edge dipoles due to subsequent motion of the remaining screw segments.

If the applied stress is greater than the passing stress for these bowed out segments, then they could easily give rise to Frank–Read sources, since the jogs are made much more stable with respect to glide. Of all the bowed out segments the most likely candidate that could give rise to Frank–Read sources is the one which has the largest spacing between the jogs. For example, this could be the end AB of the loop (Fig. 8c) where B could coincide with the crystal edge and in which case the loops give rise to single ended sources which are frequently observed earlier [8].

The analysis also shows that for the loops to act as Frank–Read sources by way of cross-slip, they should be sufficiently large. This implies that at small strains that is when the average loop size is large, the cross-slip can only lead to regeneration of dislocations and hence to further work-hardening. With increasing in strain, however, the average loop size decreases thereby decreasing, on one hand, the number of sources for dislocations due to cross-slip and increasing, on the other, the number of dislocations being annihilated due to the same cross-slip. A balance in these two factors thus sets the stage for dynamic recovery, i.e. stage III deformation.

6. Summary and conclusions

It has been shown that frictional forces are important in stabilizing dislocation loops in real crystal and further that these forces significantly affect the cross-slip and the subsequent behaviour of the dislocation loops. The critical conditions for the loops to act as Frank–Read sources in the presence of frictional forces by way of cross-slip have been determined. The results show that for the loops to act as Frank–Read sources in real crystals, the size of the loops should be sufficiently large and from this it is argued that cross-slip could lead to regeneration of dislocations at small strains. With an increasing strains, however, the number of such sources decreases while the number of dislocations being annihilated due to cross-slip increases thereby leading to stage III deformation. The ability of the loops to cross-slip under their own internal stresses could account for many experimental observations that show the presence of heavily jogged screw dislocations and the generation of dipoles of near edge orientation.

Acknowledgements

The author would like to express his sincere appreciation to Professor M. J. Marcinkowski of The Engineering Materials Group and the Department of Mechanical Engineering of The University of Maryland for a number of helpful discussions. The computer time for this investigation was made available through the facilities of the Computer Science Center of The University of Maryland. In addition, the present research effort was supported by The United States Energy Research and Development Administration under Contract No. AT-(40-1)-3935.

References

1. K. SADANANDA and M. J. MARCINKOWSKI, *J. Appl. Phys.* **43** (1972) 2609.
2. *Idem, Phys. Stat. Sol.* **a21** (1974) 581.
3. *Idem,* to be published.
4. A. H. COTTRELL, "Dislocations and Plastic Flow in Crystals" (Clarendon Press, Oxford, 1953).
5. J. S. KOEHLER, *Phys. Rev.* **86** (1952) 52.
6. J. J. GILMAN and W. G. JOHNSTON, "Dislocations and Mechanical Properties of Crystals", edited by J. C. Fisher, W. G. Johnston, R. Thomson and T. Vreeland (Wiley, New York, 1956) p. 116.
7. J. R. LOW and R. W. GUARD, *Acta Met.* **1** (1959) 171.
8. J. R. LOW and A. M. TURKALO, *ibid* **10** (1962) 215.
9. F. MINARI, B. PICHAUD and L. CAPELLA, *Phil. Mag.* **31** (1975) 275.
10. J. C. M. LI and G. C. T. LIU, "Proceedings of the International Conference on the Strength of Metals and Alloys", Suppliment to *Trans. Jap. Inst. Metals* **9** (1968) 20.
11. J. P. HIRTH and J. LOTHE, "Theory of Dislocations" (McGraw Hill, New York, 1968) p. 135.
12. T. JOSSANG, L. LOTHE and K. SKYLSTAD, *Acta Met.* **13** (1965) 297.
13. T. JOSSANG, *Phys. Stat. Sol.* **27** (1969) 579.
14. K. SADANANDA and M. J. MARCINKOWSKI, *Phys. Stat. Sol.* **a27** (1975) 141.
15. M. J. MARCINKOWSKI and D. E. CAMPBELL, "Ordered Alloys-Structural Application and Physical Metallurgy", edited by B. K. Kear, C. T. Sims, N.S. Stoloff and W. H. Westbrook (Claitor's, Baton Rouge, 1970) p. 331.
16. P. R. SWANN, "Electron Microscopy and Strength of Crystals", edited by G. Thomas and J. Washburn (Interscience, New York, 1963) p. 131.
17. A. SEEGER, "Work hardening", edited by J.P. Hirth and J. Weertman (Gordan and Breach, New York, 1968) p. 27.
18. J. T. FOURIE and H. G. F. WILSDORF, *J. Appl. Phys.* **31** (1960) 2219.
19. F. R. N. NABARRO, Z. S. BASINSKI and D. B. HOLT, *Adv. Phys.,* **13** (1964) 193.
20. P. B. PRICE, *Phil. Mag.* **5** (1960) 873.
21. *Idem, J. Appl. Phys.,* **32** (1961) 1750.
22. J. WASHBURN, *Phil. Mag.* **5** (1960) 991.
23. W. C. DASH, *J. Appl. Phys.* **29** (1958) 705.
24. A. SEEGER and S. MADER, *Phys. Stat. Sol.* **1** (1961) K78.
25. A. S. TETELMAN, *Acta Met.* **10** (1962) 813.

Received 28 April and accepted 19 May 1975.